

# Three-nucleon interactions: A frontier in nuclear structure

A. Schwenk\* and J.D. Holt

TRIUMF, 4004 Wesbrook Mall, Vancouver, BC, Canada, V6T 2A3

\*E-mail: schwenk@triumf.ca

**Abstract.** Three-nucleon interactions are a frontier in understanding and predicting the structure of strongly-interacting matter in laboratory nuclei and in the cosmos. We present results and discuss the status of first calculations with microscopic three-nucleon interactions beyond light nuclei. This coherent effort is possible due to advances based on effective field theory and renormalization group methods in nuclear physics.

The physics of strong interactions extends over extremes in density, neutron-to-proton imbalance and temperature (see Fig. 1). Understanding and predicting the properties of these fascinating forms of matter requires progress on fundamental problems in the theory of nuclear forces and in many-body physics. In this talk, we highlight the key role of three-nucleon (3N) interactions for nuclear structure.

Nuclear interactions depend on a resolution scale, which we denote by a generic momentum cutoff  $\Lambda$ , and the Hamiltonian is always given by an effective theory for nucleon-nucleon (NN) and corresponding many-nucleon interactions (with corresponding effective operators) [1, 2, 3]:

$$H(\Lambda) = T + V_{\text{NN}}(\Lambda) + V_{\text{3N}}(\Lambda) + V_{\text{4N}}(\Lambda) + \dots \quad (1)$$

This scale dependence is similar to the scale dependence of parton distribution functions, and shows that the effect of 3N interactions depends on this scale and the theoretical convention that enters all parts of the Hamiltonian.

At very low momenta  $Q \ll m_\pi \approx 140 \text{ MeV}$ , the details of pion exchanges are not resolved and nuclear forces can be systematically expanded in contact interactions and their derivatives [1]. The corresponding pionless effective field theory (EFT) is extremely successful for capturing universal large scattering-length physics (with improvements by including effective range and higher-order terms) in loosely-bound or halo nuclei, reactions at astrophysical energies and in dilute neutron matter (see e.g., Ref. [4]).

For most nuclei, the typical Fermi momenta are  $Q \sim m_\pi$  and therefore pion exchanges have to be included explicitly. In chiral EFT, nuclear interactions are then organized in an expansion in powers of  $Q/\Lambda_b$ , where  $\Lambda_b$  denotes the breakdown scale, roughly  $\Lambda_b \sim m_\rho$  [1, 2]. The great advantage is that up to next-to-next-to-next-to-leading order ( $\text{N}^3\text{LO}$ ) only two new 3N couplings enter, since parts of the 3N force can be consistently determined by  $\pi\text{N}$  and NN couplings. The two 3N couplings, as well as the short-ranged NN couplings, depend on the resolution scale  $\Lambda$  and for each  $\Lambda$  can be fit to data.

Using the renormalization group (RG), we can evolve an initial potential to lower resolution by integrating out high momenta through discretized RG flow equations

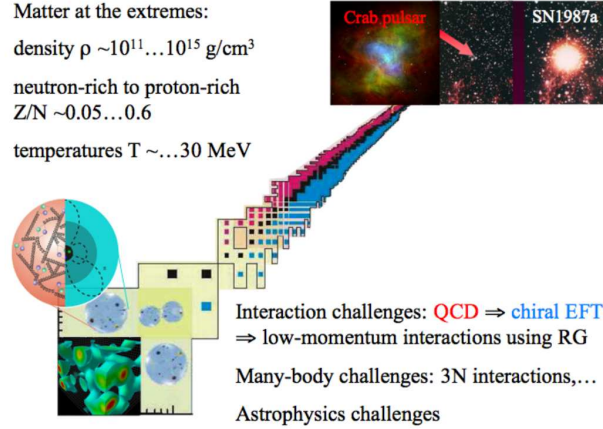


**FIGURE 1.** From the QCD vacuum to laboratory nuclei to neutron stars and supernovae.

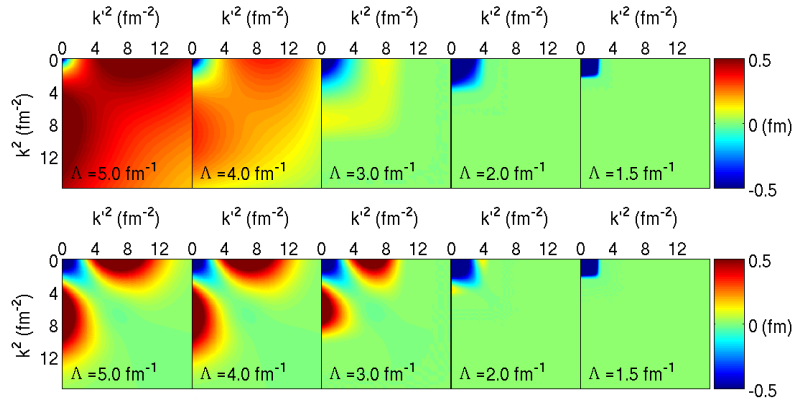


**FIGURE 2.** Evolution of the  $^3S_1$  partial wave with a smooth  $n_{\text{exp}} = 8$  regulator at cutoffs  $\Lambda = 5.0, 4.0, 3.0, 2.0$  and  $1.5 \text{ fm}^{-1}$  (for details see Ref. [6]). The initial potentials are Argonne  $v_{18}$  [11] (top) and a  $N^3\text{LO}$  chiral EFT potential from Ref. [12] (bottom). The color scale ranges from  $-0.5$  to  $0.5 \text{ fm}$ .

or equivalent Lee-Suzuki transformations [3, 5]. In the last two years, these methods have been refined to employ smooth regulators [6] and similarity renormalization group (SRG) transformations [7, 8], which both have technical advantages in oscillator spaces.

Changing the cutoff leaves observables unchanged by construction, but shifts contributions between the potential and the sums over intermediate states in loop integrals. Since the sums are restricted by the intrinsic resolution  $\Lambda$ , these shifts can weaken or largely eliminate sources of nonperturbative behavior such as strong short-range repulsion and short-range tensor forces [9, 10]. As shown in Fig. 2, the evolution leads to low-momentum interactions, generally known as “ $V_{\text{low}k}$ ”, which become universal for  $\Lambda \lesssim 2 \text{ fm}^{-1}$  and have weak off-diagonal coupling. Since the RG preserves the long-range parts of nuclear interactions [6], this leads to a weak renormalization of long-range operators, for example for the deuteron rms radius in Fig. 3.

The evolution of chiral EFT interactions to lower cutoffs is beneficial for two reasons. First, the RG generates all higher-order short-range contact interactions so that observables are exactly reproduced and the theoretical uncertainty remains at the level of the truncation error in the initial potential. We illustrate this in Fig. 4 by comparing the flow

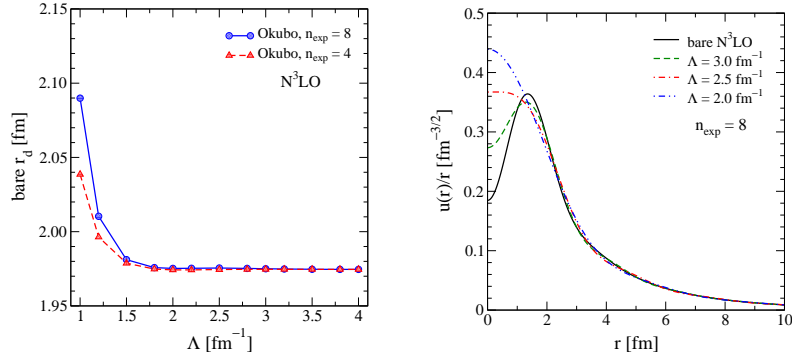


**FIGURE 3.** The deuteron rms radius  $r_d$  calculated with the bare operator as a function of the cutoff (left). The radius is only weakly dependent on the cutoff for  $\Lambda > 1.5 \text{ fm}^{-1}$ , although the intrinsic resolution in the S-state deuteron wave function changes substantially with  $\Lambda$  (right). For details see Ref. [6].

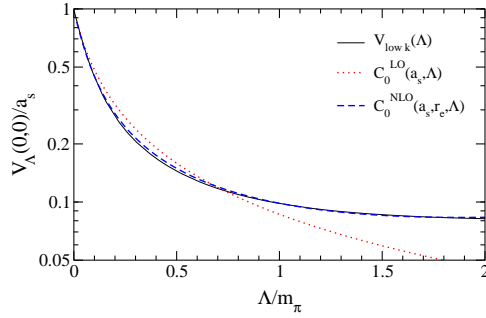


**FIGURE 4.** Flow of  $V_{\text{low}k}(k' = 0, k = 0; \Lambda)$  compared to the corresponding momentum-independent contact interaction  $C_0(\Lambda)$  at LO and NLO, where this coupling is determined entirely from RG invariance and fits to the scattering length  $a_s$  (at LO) plus effective range  $r_e$  (at NLO).

of  $V_{\text{low}k}(k' = 0, k = 0; \Lambda)$  with the corresponding momentum-independent contact interaction  $C_0(\Lambda)$  in subsequent orders of pionless EFT. Second, lower resolutions can be represented efficiently in oscillator bases, and therefore lead to direct convergence in nuclear structure calculations [6]. This is demonstrated by the very promising convergence for  $N_{\text{max}} \sim 10$  in NCSM calculations with SRG interactions [13] shown in Fig. 5.

$V_{\text{low}k}(\Lambda)$  defines a class of NN interactions with cutoff-independent low-energy NN observables. Consequently, any cutoff variation of observables estimates the truncation errors due to neglected many-body interactions in  $H(\Lambda)$  of Eq. (1). Figure 6 shows that this cutoff dependence explains the empirical Tjon line, that 3N interactions are required by renormalization and needed to break off the line to accurately describe the experimental  ${}^3\text{H}$  and  ${}^4\text{He}$  binding energies [14]. NN-only results also lead to Tjon lines in medium-mass nuclei, where results truncated in oscillator shells as well as for different  $\hbar\Omega$  lie approximately on the same lines [15].

Three-nucleon interactions are crucial for many-nucleon systems. In addition to the impact on binding energies, they play a central role for spin-orbit and spin dependences, for isospin dependences of neutron- and proton-rich systems, and they drive the density dependence of nucleonic matter. The latter are pivotal for extrapolations to the extremes of astrophysics. Three-nucleon interactions are also a frontier in few-body scattering (for a critical discussion, see e.g., Ref. [16]). Since 3N contributions are amplified in nuclei, it may be necessary for controlled predictions to constrain 3N couplings with few- and

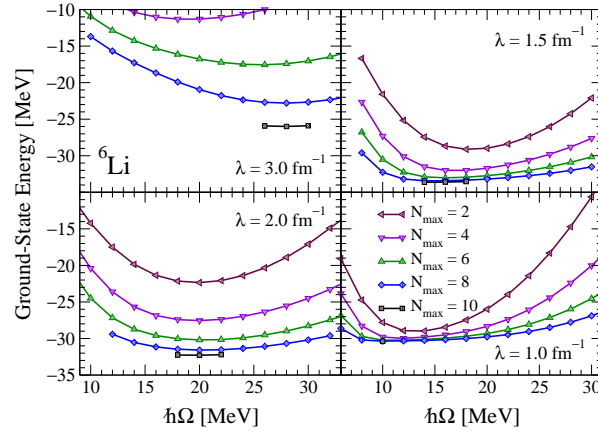


**FIGURE 5.** Ground-state energy of  ${}^6\text{Li}$  as a function of the oscillator parameter  $\hbar\Omega$  at four different values of SRG resolution  $\lambda = 3, 2, 1.5$  and  $1\text{ fm}^{-1}$ . The NCSM results clearly show improved convergence with the maximum number of oscillator quanta  $N_{\text{max}}$  for lower cutoffs. For details see Ref. [13].

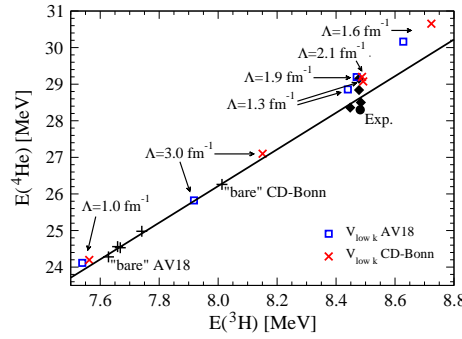


**FIGURE 6.** Correlation of the  ${}^3\text{H}$  and  ${}^4\text{He}$  binding energies. The cutoff dependence of the exact NN-only results with  $V_{\text{low}k}(\Lambda)$  explains the empirical (solid) Tjon line. For details see Ref. [14].

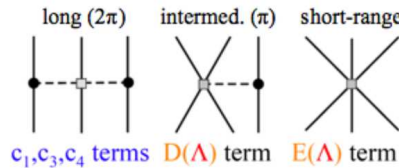


**FIGURE 7.** Leading ( $N^2\text{LO}$ ) 3N interaction in chiral EFT without explicit Deltas.

many-body data. Therefore a coherent 3N effort is needed with theoretical uncertainties.

In chiral EFT without explicit Deltas, 3N interactions start at  $N^2\text{LO}$  or order  $(Q/\Lambda_b)^3$  [1, 2] and their contributions are given diagrammatically in Fig. 7. The low-energy constants for the long-range parts relate  $\pi\text{N}$ , NN and 3N interactions, and the determination from  $\pi\text{N}$  scattering is, within errors, consistent with the extraction from peripheral NN waves. The present constraints are  $c_1 = -0.9^{+0.2}_{-0.5}$ ,  $c_3 = -4.7^{+1.2}_{-1.0}$  and  $c_4 = 3.5^{+0.5}_{-0.2}$  (all in  $\text{GeV}^{-1}$ ) [17]. In particular,  $c_3$  and  $c_4$  are important for nuclear structure and have large uncertainties (see Fig. 11 for the impact on nucleonic matter).

For lower cutoffs, we take the corresponding 3N interactions  $V_{3\text{N}}(\Lambda)$  from chiral EFT by fitting the D- and E-term couplings to the  ${}^3\text{H}$  and  ${}^4\text{He}$  binding energies for a range of cutoffs [14]. Since chiral EFT is a complete basis, this gives the 3N force up to

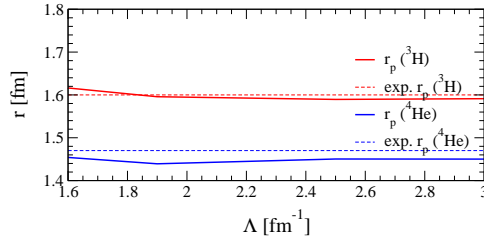


**FIGURE 8.** The  ${}^3\text{H}$  and  ${}^4\text{He}$  radii are approx. cutoff independent with NN and 3N interactions [18].

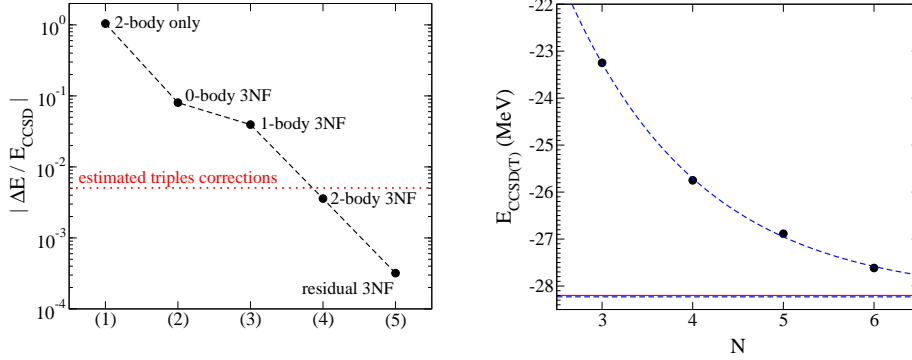


**FIGURE 9.** Relative contributions  $|\Delta E/E|$  to the binding energy of  ${}^4\text{He}$  at the CCSD level from  $V_{lowk}$  as well as normal-ordered 0-, 1-, 2-body and residual 3-body parts of the 3N interaction (left). Convergence of the corresponding CCSD(T) results with the number of oscillator shells (right). The extrapolated binding energy  $-28.23\text{ MeV}$  agrees well with the exact result  $-28.20(5)\text{ MeV}$ . For details see Ref. [19].

truncation errors. We have found that the resulting 3N interactions become perturbative for  $\Lambda \lesssim 2\text{ fm}^{-1}$ , while they are nonperturbative for larger cutoffs, and that the size of 3N expectation values is natural  $\sim (Q/\Lambda_b)^3 \langle V_{lowk} \rangle$  [14].

As for the Tjon line, cutoff variation can provide lower bounds for theoretical uncertainties due to neglected many-body interactions or an incomplete many-body treatment. As shown in Fig. 8, this is a powerful and practical tool, which is important for extrapolations, in particular for matrix elements needed in fundamental symmetry tests (e.g., double-beta decay and isospin-violating corrections for super-allowed beta decay).

Coupled-cluster (CC) theory combined with rapid convergence for low-momentum interactions pushes the limits of accurate calculations to medium-mass nuclei and sets new benchmarks for  ${}^{16}\text{O}$  and  ${}^{40}\text{Ca}$  [19]. In Fig. 9, first CC results with 3N forces show that low-momentum 3N interactions are accurately treated as effective 0-, 1- and 2-body terms, and that residual 3N interactions can be neglected [19]. This is very promising and supports the idea that phenomenological monopole shifts in shell model interactions are due to 3N contributions [20], see also the talk by T. Otsuka and Ref. [21]. This links understanding the shell model and the drip lines to 3N forces. First investigations in this direction are presented in Fig. 10 [22]. We speculate that the  $T = 0$  monopoles with large cutoff dependences receive cutoff-dependent contributions mainly from second-order NN-3N terms (which are expected to be attractive) and that the  $T = 1$  monopoles receive cutoff-independent contributions from the 3N  $c_i$  terms (which are repulsive in nuclear matter). Systematic investigations of 3N forces and valence-shell interactions are in progress [22].

Finally, there is the possibility of perturbative nuclear matter with low-momentum

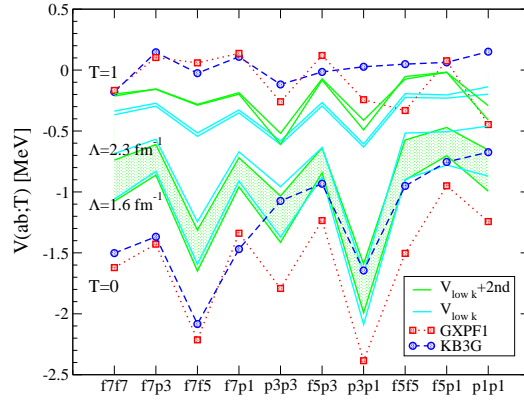


**FIGURE 10.** Monopole interactions in the pf shell obtained from  $V_{\text{low}k}$  plus second-order many-body contributions for a range of cutoffs, compared to phenomenological matrix elements [22].

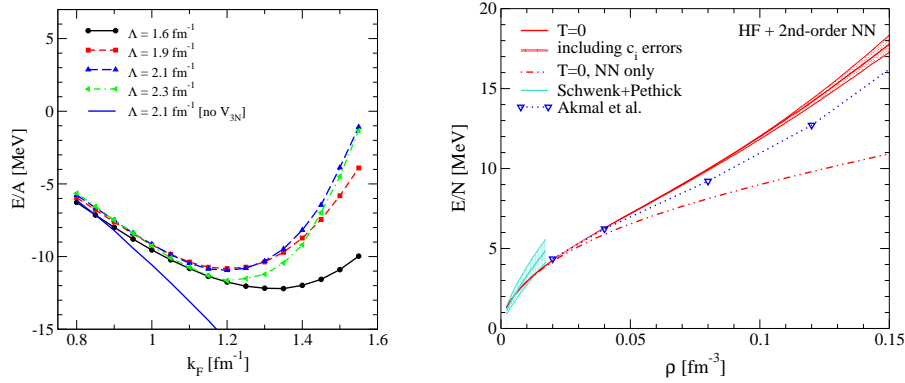


**FIGURE 11.** Nuclear (left) and neutron matter (right) from low-momentum NN and 3N interactions based on Hartree-Fock plus dominant second-order contributions for various cutoffs. For details see Ref. [9, 23].

NN and 3N interactions [9]. As shown in Fig. 11, with second-order contributions the cutoff dependence is very weak at low densities. We have found that 3N forces drive saturation [9], and at present the uncertainties in the  $c_i$  overwhelm other uncertainties (see the results for neutron matter) [23]. Lower values for  $c_3$  (as also expected from  $N^3\text{LO}$  3N terms) add  $\approx -2$  MeV at saturation density in neutron matter, and this also corresponds to the value from Delta resonance saturation (which explains the agreement with the results of Akmal et al.). These findings will provide guidance for constructing a universal density functional for nuclei. Towards denser matter, 4N force contributions of  $E/A \sim 1$  MeV would not be unreasonable.

This is an exciting era: with advances on many fronts, a coherent effort to understand and predict nuclear systems based on effective field theory and renormalization group interactions, where 3N forces are a frontier.

It is a pleasure to thank the organizers for a very stimulating FM50 conference and the collaborators who have contributed to these results: S. Bogner, G. Brown, D. Dean, B. Friman, R. Furnstahl, G. Hagen, T. Kuo, P. Maris, A. Nogga, T. Papenbrock, R. Perry, L. Tolos, J. Vary and A. Zuker. This work was supported by NSERC. TRIUMF receives federal funding via a contribution agreement through the NRC of Canada.

## REFERENCES

1. P.F. Bedaque and U. van Kolck, *Ann. Rev. Nucl. Part. Sci.* **52**, 339 (2002).
2. E. Epelbaum, *Prog. Part. Nucl. Phys.* **57**, 654 (2006).
3. S.K. Bogner, T.T.S. Kuo and A. Schwenk, *Phys. Rept.* **386**, 1 (2003).
4. A. Schwenk and C.J. Pethick, *Phys. Rev. Lett.* **95**, 160401 (2005).
5. S.K. Bogner, A. Schwenk, T.T.S. Kuo and G.E. Brown, nucl-th/0111042.
6. S.K. Bogner, R.J. Furnstahl, S. Ramanan and A. Schwenk, *Nucl. Phys. A* **784**, 79 (2007).
7. S.K. Bogner, R.J. Furnstahl and R.J. Perry, *Phys. Rev. C* **75**, 061001(R) (2007).
8. S.K. Bogner et al., *Phys. Rev. C* in press, arXiv:0801.1098.
9. S.K. Bogner, A. Schwenk, R.J. Furnstahl and A. Nogga, *Nucl. Phys. A* **763**, 59 (2005).
10. S.K. Bogner, R.J. Furnstahl, S. Ramanan and A. Schwenk, *Nucl. Phys. A* **773**, 203 (2006).
11. R.B. Wiringa, V.G.J. Stoks and R. Schiavilla, *Phys. Rev. C* **51**, 38 (1995).
12. D.R. Entem and R. Machleidt, *Phys. Rev. C* **68**, 041001(R) (2003).
13. S.K. Bogner et al., *Nucl. Phys. A* **801**, 21 (2008).
14. A. Nogga, S.K. Bogner and A. Schwenk, *Phys. Rev. C* **70**, 061002(R) (2004).
15. G. Hagen, D.J. Dean and A. Schwenk, in prep.
16. H.-O. Meyer, TRIUMF 3N Workshop (2007), see <http://www.triumf.info/hosted/TNI/index.html>.
17. U.G. Meißner, private comm. (2007).
18. A. Nogga, private comm. (2004).
19. G. Hagen et al., *Phys. Rev. C* **76**, 034302 (2007); *ibid.*, **76**, 044305 (2007).
20. A.P. Zuker, *Phys. Rev. Lett.* **90**, 042502 (2003).
21. A. Schwenk and A.P. Zuker, *Phys. Rev. C* **74**, 061302(R) (2006).
22. J.D. Holt and A. Schwenk, in prep.
23. L. Tolos, B. Friman and A. Schwenk, arXiv:0711.3613.